Fermion-spin transformation to implement the charge-spin separation

Shiping Feng
International Centre for Theoretical Physics, P.O. Box 586, 34100 Trieste, Italy
and Department of Physics, Beijing Normal University, Beijing 100875, China

Z. B. Su
Institute of Theoretical Physics, Chinese Academy of Sciences, Beijing 100080, China
and International Centre for Theoretical Physics, P.O. Box 586, 34100 Trieste, Italy

L. Yu
International Centre for Theoretical Physics, P.O. Box 586, 34100 Trieste, Italy
and Institute of Theoretical Physics, Chinese Academy of Sciences, Beijing 100080, China
(Received 2 February 1993; revised manuscript received 21 July 1993)

A fermion-spin transformation is used to implement the charge-spin separation, and is developed to study the low-dimensional t-J model. In this approach, the charge and spin degrees of freedom of the physical electron are separated, and the charge degree of freedom is represented by a spinless fermion while the spin degree of freedom is represented by a hard-core boson. The on-site local constraint for single occupancy is satisfied even in the mean-field approximation and the sum rule for the physical electron is obeyed. This approach can be applied to both one and two-dimensional systems. In the one-dimensional case, the spinon as well as the physical electron behave like Luttinger liquids. We have obtained a gapless charge and spin excitation spectrum, a good ground state energy, and a reasonable electron-momentum distribution within the mean-field approximation. The correct exponents of the correlation functions and momentum distribution are also obtained if the squeezing effect and rearrangement of the spin configurations are taken into account. In the two-dimensional case, within the mean-field approximation the magnetized flux state with a gap in the spinon spectrum has the lowest energy at half-filling. The antiferromagnetic long-range order is destroyed by hole doping of the order $\sim 10-15\,\%$ for $t/J=3-5$ and a disordered flux state with gapless spinon spectrum becomes stable. The calculated specific heat is roughly consistent with observed results on copper oxide superconductors. The possible phase separation is also discussed at the mean-field level.

I. INTRODUCTION

The large-U Hubbard model and its equivalent, the t-J model, are prototypes to study strong correlation effects in solids, especially in connection with the high-T_c superconductivity.[1–3] The central issue under debate is whether the non-Fermi-liquid behavior, showing up as charge-spin separation and vanishing of the quasiparticle residue, inherent to the one-dimensional (1D) Hubbard model, is also true for two-dimensional (2D) models, as conjectured by Anderson.[4]

In 1D, the exact Bethe-ansatz solutions[5,6] are available for the t-J model in the limit $J/t\to 0$ and $J/t=2$. The Hubbard model and the t-J model in the small-J limit scale to the Luttinger model.[5,7,8] Using Lieb-Wu's exact wave function, Ogata and Shiba[5] have shown the existence of an electron Fermi surface as well as a singular behavior at $k\sim k_F$ and $k\sim 3k_F$ in the electron-momentum distribution function. Moreover, Yokoyama and Ogata[9] and Assaad and Würtz[10] have studied the 1D t-J model using the exact diagonalization of small systems and quantum Monte Carlo methods, respectively, and their results show that the t-J model behaves like a Luttinger liquid for low values of J/t, and undergoes phase separation at large values of J/t. Hellberg and Mele[11] came to the same conclusion by using the Jastrow variational wave function. Thus the typical behavior of the Luttinger liquid[12] in 1D, i.e., the absence of quasiparticle propagation and charge-spin separation, has been demonstrated explicitly for the t-J model in the small-J limit.

There are no exact solutions available in 2D. The variational calculations[13] seem to support Anderson's conjecture. The quantum Monte Carlo simulations gave some hint at the vanishing of the quasiparticle residue in the thermodynamic limit.[14] However, this result is not conclusive because of the "fermion minus sign" problem in the Monte Carlo technique and contrary results in exact diagonalization of clusters[15] as well as analytic treatments of the single-hole problem.[16]

The crucial requirement[17] for the t-J model (and the large-U Hubbard model) is to impose the single occupancy constraint $\sum_\sigma C^\dagger_{i\sigma}C_{i\sigma}\leq 1$. An intuitively appealing approach to implement this constraint and the charge-spin separation scheme is the slave particle formalism,[18,3] where the electron operator is decomposed as $C_{i\sigma}=a^\dagger_i f_{i\sigma}$ with $a^\dagger_i$ as the slave boson and $f_{i\sigma}$ as the fermion and the local constraint $\sum_\sigma f^\dagger_{i\sigma}f_{i\sigma}+a^\dagger_i a_i=1$, or *vice versa*, i.e., $a^\dagger_i$ as fermion and $f_{i\sigma}$ as boson. Due

to the constraint, these particles are also coupled by a strong gauge field,[19] allowed by this slave-particle representation. In the mean-field approximation (MFA) the spin (spinons) and charge (holons) degrees of freedom are fully separated. However, there are a number of difficulties in this approach. First of all, in the slave-boson version, the antiferromagnetic correlation is absent for zero doping, so the ground state energy in the 2D case is high compared with the numerical estimate for small clusters, and the Marshall sign rule[20] is not obeyed.[21,22] Alternatively, in the slave-fermion approach, the ground state is antiferromagnetic for the undoped case and persists until very high doping (~ 60 %).[23] The large Fermi surface of spinons, present in the slave-boson approach, is absent there. Moreover, if, following the common practice, we let $f_{i\sigma}$ keep track of the spin, while letting a_i keep track of the charge, satisfying the sum rules: $\delta = \langle a_i^\dagger a_i \rangle$ and $1-\delta = \sum_\sigma \langle f_{i\sigma}^\dagger f_{i\sigma} \rangle$, where δ is the hole doping concentration, we find[24] that the sum rule for the physical electron $\sum_\sigma \langle C_{i\sigma}^\dagger C_{i\sigma} \rangle = 1 - \delta$ is not satisfied for both versions. This expectation value is $(1-\delta)^2$ in the slave-fermion representation, and $1-\delta^2$ in the slave-boson version. Since the total number of particles does not depend on the interactions, this difficulty will persist even beyond the MFA, so long as the spinon and holon expectation value decoupling is assumed. Furthermore, we have also shown[24] that the overall electron distribution does not have the appropriate Fermi surface within this scheme even for the 1D case. These are intrinsic difficulties of this decoupling scheme.

In this paper we develop another scheme, the fermion-spin transformation, to implement the local constraint and the charge-spin separation. In this scheme the charge degree of freedom is represented by a spinless fermion, while the spin degree of freedom is represented by a *hard-core* boson in terms of Pauli operators (with a projection operator to be specified later). Using this representation the local constraint is satisfied in the decoupling scheme in contrast with the existing slave particle approach,[18,3] where the local constraint is replaced by a global one. As a consequence, the sum rule for the physical electron is obeyed. Moreover, the *hard-core* bosons can be expressed in terms of spinless fermions via the Jordan-Wigner transformation in 1D (Ref. 25) and its generalization in 2D.[26] This is an efficient calculation scheme which can provide very good results even at the mean-field level.

Here we summarize our main results. In 1D we can integrate out the spinless charge field (holons) and obtain an effective Hamiltonian for an interacting spinon field which behaves like a Luttinger liquid. Hence the physical electron, as a convolution of spinon and holon, also behaves like a Luttinger liquid in consistency with the exact solution.[5] Moreover, we obtain a gapless spectrum for both holons and spinons at the mean-field level which is not true in the slave-fermion approach. The ground state energy at and away from half-filling is in good agreement with exact results. By going beyond the MFA to include the "squeezing" effect and rearrangement of the spin configurations due to the hole presence, we obtain not only correct exponents of correlation functions and momentum distribution at the Fermi surface but also a reasonable global distribution function. In 2D we have considered various phases at and away from half-filling in the MFA. The magnetized flux state with a gap in the spinon spectrum has the lowest energy at half-filling. The antiferromagnetic long-range order (AFLRO) fades away by hole doping of the order $10-15$ % for $t/J = 3-5$ in contrast to the Schwinger boson approach where the AFLRO is destroyed at 62% doping.[23] Beyond the critical concentration, a disordered flux phase with a gapless spectrum becomes stable. We have also calculated the specific heat and considered the phase separation issue. The results are consistent with experiments and numerical simulations, respectively.

The rest of the paper is organized as follows: In Sec. II, we explain in detail the fermion-spin transformation which is exact in the single occupancy Hilbert space, if a projection operator is introduced to remove the extra degrees of freedom. We also estimate the errors introduced by the MFA. In Sec. III we apply the proposed scheme to the 1D t-J model within the MFA. The main results obtained have been mentioned above. In Sec. IV we calculate the correlation functions and momentum distribution by introducing two "string" operators which take care of the squeezing effect and rearrangement of the spin configurations. The exponents thus obtained agree with the exact results. The applications to 2D at the mean-field level are described in Sec. V. Finally, in the concluding section we make some further remarks to explain our current understanding why this simple transformation works so well and outline some open problems.

II. FERMION-SPIN TRANSFORMATION TO IMPLEMENT THE CHARGE-SPIN SEPARATION

A. Model, constraints, and sum rules

We start from the t-J model which can be written as

$$H = -t \sum_{\langle ij \rangle \sigma} (C_{i\sigma}^\dagger C_{j\sigma} + \text{H.c.}) - \mu \sum_{i\sigma} C_{i\sigma}^\dagger C_{i\sigma} + J \sum_{\langle ij \rangle} \mathbf{S}_i \cdot \mathbf{S}_j, \tag{1}$$

where $C_{i\sigma}^\dagger$ ($C_{i\sigma}$) are the electron creation (annihilation) operators, $\mathbf{S}_i = C_i^\dagger \sigma C_i/2$ spin operators with σ as Pauli matrices, and μ is the chemical potential. The summation $\langle ij \rangle$ is carried over nearest neighbor nonrepeated bonds.

The Hamiltonian (1) is defined in a restricted Hilbert space without double electron occupancy. There are two ways to implement this requirement: either to solve (1) combined with a nonholonomic constraint $\sum_\sigma C_{i\sigma}^\dagger C_{i\sigma} \leq 1$ or to introduce constrained fermion operators,[27] replacing $C_{i\sigma}$ by $\tilde{C}_{i\sigma} = C_{i\sigma}(1 - n_{i\bar{\sigma}})$, where $n_{i\sigma} = C_{i\sigma}^\dagger C_{i\sigma}$. We will use both representations in this paper.

The constrained operators $\tilde{C}_{i\sigma}$ satisfy the following relations:

$$\sum_\sigma \tilde{C}^\dagger_{i\sigma}\tilde{C}_{i\sigma} = \sum_\sigma C^\dagger_{i\sigma}C_{i\sigma}(1-n_{i\bar{\sigma}}),$$
$$\left\langle \sum_\sigma \tilde{C}^\dagger_{i\sigma}\tilde{C}_{i\sigma}\right\rangle = 1-\delta, \tag{2}$$

where the latter equation is a sum rule for the electron at the hole doping concentration δ, and $\langle\cdots\rangle$ means the thermodynamical average. The on-site anticommutation relation of the constrained electron operator $\tilde{C}_{i\sigma}$ is

$$\sum_\sigma \{\tilde{C}_{i\sigma}, \tilde{C}^\dagger_{i\sigma}\} = 2 - \sum_\sigma C^\dagger_{i\sigma}C_{i\sigma},$$
$$\left\langle \sum_\sigma \{\tilde{C}_{i\sigma}, \tilde{C}^\dagger_{i\sigma}\}\right\rangle = 1+\delta, \tag{3}$$

which gives rise to a sum rule for the spectral function $A_{c\sigma}(k,w)$,

$$\sum_\sigma \int_{-\infty}^{\infty} \frac{dw}{2\pi} A_{c\sigma}(k,w) = 1+\delta. \tag{4}$$

Of course, this value is less than 2 since $1-\delta$ states are pushed to infinity as $U\to\infty$ in deriving the t-J model. Hence the electron spectral function $A_{c\sigma}(k,w)$ describes only the lower Hubbard band. Equations (2) and (4) are exact sum rules for the t-J model, and they must be preserved in adequate treatments.

B. CP^1 hard-core boson

The decoupling of the charge and spin degrees of freedom for the physical electron is undoubtedly correct in the 1D t-J model,[5] but the situation is still not clear in 2D. In this paper, we presume that the decoupling of charge and spin degrees of freedom for the physical electron is also valid for the 2D t-J model, and we propose another scheme to decouple the charge and spin degrees of freedom.

To motivate this transformation, we start from the no-double occupancy local constraint $\sum_\sigma C^\dagger_{i\sigma}C_{i\sigma}\le 1$. Supposing $C_{i\sigma} = h^\dagger_i b_{i\sigma}$ with the spinless fermion operator h_i keeping track of the charge (holon) while the operator $b_{i\sigma}$ keeping track of the spin (spinon), then this on-site local constraint can be rewritten as $\sum_\sigma h_i h^\dagger_i b^\dagger_{i\sigma}b_{i\sigma}\le 1$. Since the electron obeys the Fermi statistics, the operator $b_{i\sigma}$ must be a boson when the operator h_i has been assigned a fermion character in this electron decoupling scheme. If bosons are subject to the condition $\sum_\sigma b^\dagger_{i\sigma}b_{i\sigma}=1$, the on-site electron local constraint

$$n_c = \sum_\sigma C^\dagger_{i\sigma}C_{i\sigma} = h_i h^\dagger_i = 1 - h^\dagger_i h_i \le 1 \tag{5}$$

is exactly satisfied, where $n_h = h^\dagger_i h_i$ is the spinless holon number at site i, equal to 1 or 0. This way the non-holonomic on-site electron constraint is converted into a holonomic boson constraint.

We should note that so long as $h^\dagger_i h_i = 1$, $\sum_\sigma C^\dagger_{i\sigma}C_{i\sigma} = 0$, no matter what the value of $n_b = \sum_\sigma b^\dagger_{i\sigma}b_{i\sigma}$ is. However, the choice $n_b = 1$ is convenient, because it also guarantees the condition $n_c = 1$, when $n_h = 0$. This decoupling scheme, the so-called CP^1 representation, was proposed by Wiegmann[28] and was used in Ref. 29. The constraint $n_c = 1$ means the presence of one boson (spin-up or -down) on each site, i.e., we assign a "spin" even to an empty site. This will not affect the physical expectation values, because the hole number expectation $\langle n_h\rangle$ will remove the spurious effects. Nevertheless, the extra degrees of freedom will affect the partition function and thermodynamical quantities. In the next subsection we will define a projection operator to cure this defect. As a result, the commutation relations and sum rules (2)–(4) will be satisfied exactly.

Now we explore further the properties of the CP^1 bosons. First note that if we restrict the boson occupation number to 0 or 1, the infinite-dimensional Fock space for bosons becomes two-dimensional, where we can choose the following representation:

$$b_i = \begin{pmatrix} 0 & 0 \\ 1 & 0 \end{pmatrix}, \quad b^\dagger_i = \begin{pmatrix} 0 & 1 \\ 0 & 0 \end{pmatrix}, \tag{6}$$

which are nothing but spin-lowering S^- and spin-raising S^+ operators for $S=1/2$ and satisfy the *hard-core* constraints $bb = b^\dagger b^\dagger = 0$.

Moreover, if we request that $\uparrow$ and $\downarrow$ *hard-core* bosons satisfy the CP^1 condition $n_b = 1$, the 2×2 representation space becomes two-dimensional. Assume $\binom{1}{0}_\uparrow$, $\binom{0}{1}_\uparrow$ are singly occupied and empty spin-up, while $\binom{0}{1}_\downarrow$, $\binom{1}{0}_\downarrow$ are singly occupied and empty spin-down states, respectively. Due to the constraint $b^\dagger_{i\uparrow}b_{i\uparrow} + b^\dagger_{i\downarrow}b_{i\downarrow} = 1$, out of four possible states as direct products, only two, namely $\binom{1}{0}_\uparrow\binom{1}{0}_\downarrow$ and $\binom{0}{1}_\uparrow\binom{0}{1}_\downarrow$, are allowed. Thus we can ignore the spin label in the state and represent $b_\uparrow$ as $\left(\begin{smallmatrix}0&0\\1&0\end{smallmatrix}\right)$, and $b_\downarrow$ as $\left(\begin{smallmatrix}0&1\\0&0\end{smallmatrix}\right)$ in the reduced two-dimensional representation space. Of course, all the *hard-core boson* conditions, i.e., $b_{i\sigma}b^\dagger_{i\sigma} + b^\dagger_{i\sigma}b_{i\sigma} = 1$, $b^\dagger_{i\sigma}b^\dagger_{i\sigma} = b_{i\sigma}b_{i\sigma} = 0$ (without summation over σ), are satisfied. As a result, $b_\uparrow$ and $b_\downarrow$ are identified with the spin lowering S^- and raising S^+ operators, respectively, while the boson occupation space is identified with the spin-$\frac{1}{2}$ representation space.

To sum up, as solutions of the single occupancy constraint $\sum_\sigma C^\dagger_{i\sigma}C_{i\sigma}\le 1$ under CP^1 convention $\sum_\sigma b^\dagger_{i\sigma}b_{i\sigma}=1$, we find the following fermion-spin transformation:

$$C_{i\uparrow} = h^\dagger_i S^-_i, \quad C_{i\downarrow} = h^\dagger_i S^+_i \tag{7}$$

in terms of which the t-J Hamiltonian (1) can be rewritten as

$$H = -t\sum_{\langle ij\rangle\sigma} h_i h^\dagger_j (S^+_i S^-_j + S^-_i S^+_j) + \text{H.c.}$$
$$-\mu\sum_i h_i h^\dagger_i + J\sum_{\langle ij\rangle}(1-h^\dagger_i h_i)\mathbf{S}_i\cdot\mathbf{S}_j(1-h^\dagger_j h_j), \tag{8}$$

where $\mathbf{S}_i$ is the *pseudospin* operator at site i which can be expressed as CP^1 hard-core bosons and is different from the *electron spin* operator in Eq. (1). We would empha-

size that the present CP^1 hard-core boson representation of spin operators is different from the CP^1 boson representation of the spin operator used before.[28,29] In their approach, the spin degree of freedom is represented by ordinary boson operators, while, in the present scheme, the hard-core boson operator $b_{i\sigma}$ behaves as a fermion on the same site, and as a boson on different sites.

C. Projection operator

In the local representation the restricted Hilbert space of no-double occupancy consists of three states, $|0\rangle$, $|\uparrow\rangle$, $|\downarrow\rangle$, while in the fermion-spin transformation presented in the previous subsection there are four states $|\text{hole}\rangle \otimes |\text{spin}\rangle$, namely $|1,\uparrow\rangle$, $|1,\downarrow\rangle$, $|0,\uparrow\rangle$, and $|0,\downarrow\rangle$, where 1 or 0 means hole occupation. We can introduce a projection operator P to remove the extra degrees of freedom. The matrix elements of this operator can be defined as

$$P_{\kappa\alpha} \equiv |\kappa\rangle\langle\alpha|, \tag{9}$$

where $|\kappa\rangle$ is one of the bases of the physical states, while $|\alpha\rangle$ is one of the bases in the space $|\text{hole}\rangle \otimes |\text{spin}\rangle$. Since the space dimensions of $|\kappa\rangle$ and $|\alpha\rangle$ are different, the usual relations for the projection operator $P^2 = P = P^\dagger$ are not satisfied. Using this operator, one can define the electron operators in the constrained space as

$$\begin{aligned} \tilde{C}_{i\uparrow} &= P_i h_i^\dagger S_i^- P_i^\dagger, \quad \tilde{C}_{i\downarrow} = P_i h_i^\dagger S_i^+ P_i^\dagger, \\ \tilde{C}_{i\uparrow}^\dagger &= P_i h_i S_i^+ P_i^\dagger, \quad \tilde{C}_{i\downarrow}^\dagger = P_i h_i S_i^- P_i^\dagger, \end{aligned} \tag{10}$$

where P_i is the projection operator for the site i, and $P_i^\dagger$ is the Hermitian conjugate of P_i. Making use of the matrix representation of the holon operator $h_i^\dagger = \left(\begin{smallmatrix} 0 & 1 \\ 0 & 0 \end{smallmatrix}\right)$, $h_i = \left(\begin{smallmatrix} 0 & 0 \\ 1 & 0 \end{smallmatrix}\right)$, we can write down explicitly all these operators in matrix form (see the Appendix). In particular, the constrained electron operators in the basis of the physical states $|0\rangle$, $|\uparrow\rangle$, $|\downarrow\rangle$ can be written as

$$\begin{aligned} \tilde{C}_{i\uparrow} &= \begin{pmatrix} 0 & 1 & 0 \\ 0 & 0 & 0 \\ 0 & 0 & 0 \end{pmatrix}, \quad \tilde{C}_{i\uparrow}^\dagger = \begin{pmatrix} 0 & 0 & 0 \\ 1 & 0 & 0 \\ 0 & 0 & 0 \end{pmatrix}, \\ \tilde{C}_{i\downarrow} &= \begin{pmatrix} 0 & 0 & 1 \\ 0 & 0 & 0 \\ 0 & 0 & 0 \end{pmatrix}, \quad \tilde{C}_{i\downarrow}^\dagger = \begin{pmatrix} 0 & 0 & 0 \\ 0 & 0 & 0 \\ 1 & 0 & 0 \end{pmatrix}, \end{aligned} \tag{11}$$

which are nothing but the Hubbard X operators $X_{0\uparrow}$, $X_{0\downarrow}$, etc.[30] It is then straightforward to check that

$$\sum_\sigma \tilde{C}_{i\sigma}^\dagger \tilde{C}_{i\sigma} = 1 - n_h, \tag{12}$$

$$\sum_\sigma \{\tilde{C}_{i\sigma}, \tilde{C}_{i\sigma}^\dagger\} = 1 + n_h, \tag{13}$$

where

$$n_h = \begin{pmatrix} 1 & 0 & 0 \\ 0 & 0 & 0 \\ 0 & 0 & 0 \end{pmatrix}$$

is the hole number operator. Taking expectation values of Eqs. (12) and (13), one sees immediately that the sum rules (2) and (4) are exactly satisfied. Thus we have shown that the fermion-spin transformation defined with an additional projection operator P satisfies exactly the no-double-occupancy constraint and all sum rules, i.e., they are an exact mapping.

However, the projection operator P is cumbersome to handle and in many cases, for example in the mean-field treatment of Secs. III–V, we will drop it. Now let us see which of these properties are still preserved and what kind of errors we are committing in such approximate treatments. First of all, the local constraints are exactly obeyed even in the MFA. Second, those expectation values of electron operators, including spin-spin correlation functions, which should vanish, actually do not appear due to the presence of the holon number operator $n_h = h_i^\dagger h_i$. Furthermore, as we will see later, the sum rules for the physical electron are also satisfied in the MFA. By adding an extra spin degree of freedom to an empty site we are making errors of the order δ in counting the number of states, which is negligible if $\delta \to 0$. For comparison we should note that in the usual slave-particle approach,[18] the local constraint is explicitly replaced by a global constraint in the MFA, and therefore the representation space is much larger than the representation space for the physical electron, which leads to some unphysical results.[17,24] From this point of view, our treatment of constraints for the physical electron is much better than the slave-particle approach, and therefore we believe the mean-field result based on the fermion-spin approach even without the projection operator should be better than those obtained by using the slave-particle mean-field theory. This is indeed confirmed by the mean-field calculations presented in the following sections.

We note that a similar transformation has been discussed in Ref. 31, but these authors did not stick to the single-occupancy constraints in their actual calculations.

III. THE MEAN-FIELD THEORY IN 1D WITHIN THE FERMION-SPIN APPROACH

Since an exact solution[32] for the Hubbard model (hence for the $J/t \to 0$ limit of the t-J model) is available in 1D, it is important to confront any approximate treatment with this solution. In this section we consider the 1D t-J model, using the fermion-spin transformation described in the previous section at the mean-field level, neglecting the effects of the projection operator P. As mentioned in the Introduction, the 1D t-J model exhibits a Luttinger liquid behavior, including charge-spin separation, vanishing of the quasiparticle residue, etc. We should also mention that both spin and charge excitations are gapless in 1D.[5] In the standard slave-particle approach, many of these properties are not preserved. For example, in the slave-boson case[33] there is a Bose condensation at the mean-field level which leads to a Fermi-liquid behavior. On the other hand, there is a gap in the spin excitation spectrum in 1D within the slave-fermion framework, even at half-filling.[23] Now consider the mean-field results in the fermion-spin approach.

A. Luttinger liquid behavior

In the fermion-spin representation, the 1D t-J model may be written as

$$H = -t\sum_i a_i^\dagger a_{i+1}(S_i^+ S_{i+1}^- + S_i^- S_{i+1}^+) + \text{H.c.} - \mu\sum_i a_i^\dagger a_i + J\sum_{\langle ij\rangle}(a_i^\dagger a_i)(\mathbf{S}_i\cdot\mathbf{S}_j)(a_j^\dagger a_j), \quad (14)$$

where, for the convenience of the following discussion, we have introduced the particle operators a_i and $a_i^\dagger$ defined as

$$a_i = h_i^\dagger, \qquad a_i^\dagger = h_i. \quad (15)$$

In the 1D case, the *hard-core bosons* S_i^+ and S_i^- can be mapped exactly onto spinless fermions using the Jordan-Wigner[25] transformation

$$S_i^+ = f_i^\dagger e^{i\pi\sum_{l<i} f_l^\dagger f_l}, \quad (16)$$

$$S_i^- = f_i e^{-i\pi\sum_{l<i} f_l^\dagger f_l}, \quad (17)$$

$$S_i^Z = f_i^\dagger f_i - \frac{1}{2}, \quad (18)$$

where f_i is the spinless fermion operator. Substituting Eqs. (16)–(18) into Eq. (14), the t-J Hamiltonian (14) can be expressed as

$$H = -t\sum_i (a_i^\dagger a_{i+1} + a_{i+1}^\dagger a_i)(f_i^\dagger f_{i+1} + f_{i+1}^\dagger f_i) - \mu\sum_i a_i^\dagger a_i + J\sum_{\langle ij\rangle} a_i^\dagger a_i[\tfrac{1}{2}(f_i^\dagger f_j + f_j^\dagger f_i) + (f_i^\dagger f_i - \tfrac{1}{2})(f_j^\dagger f_j - \tfrac{1}{2})]a_j^\dagger a_j. \quad (19)$$

We can now employ the path-integral representation in which the Lagrangian L and the partition function Z of the t-J model in the imaginary time τ can be expressed as

$$L = \sum_i a_i^\dagger \partial_\tau a_i + \sum_i f_i^\dagger \partial_\tau f_i + H, \quad (20)$$

$$Z = \int DaDa^\dagger DfDf^\dagger e^{-\int d\tau L(\tau)}. \quad (21)$$

Integrating out the spinless charge field a_i of the t-J model, we obtain an interacting spinon system, which, like any interacting fermion systems in 1D, is described by a Luttinger liquid theory.[12,34] Moreover, the physical electron as a convolution of spinon and holon also behaves like a Luttinger liquid, which means that the electron wave function renormalization constant $Z = 0$ in the 1D t-J model.

In the path-integral representation, one can introduce a $SU(2)$-invariant Hubbard-Stratonovich transformation to decouple the Lagrangian (20) by using the following auxiliary fields

$$\chi_{i,i+\eta} = S_i^+ S_{i+\eta}^-, \quad (22)$$

$$\phi_{i,i+\eta} = a_i^\dagger a_{i+\eta}, \quad (23)$$

where $\eta = \pm 1$. Note the auxiliary field $\chi_{i,i+\eta}$ is a boson type field. The MFA to the t-J model (19) is just the saddle point solution of the Lagrangian (20), i.e., the auxiliary fields $\chi_{i,i+\eta}$ and $\phi_{i,i+\eta}$ are replaced by their mean-field values $\chi_{i,i+\eta} = \chi$ and $\phi_{i,i+\eta} = \phi$, respectively, and the Hamiltonian (19) can be diagonalized as

$$H = \sum_k \varepsilon(k)a_k^\dagger a_k + \sum_k \omega(k) f_k^\dagger f_k + 4Nt\chi\phi + 2NJ[(1-\delta)^2 - \phi^2]\chi^2, \quad (24)$$

where N is the number of sites, and

$$\varepsilon(k) = -4t\chi\cos(k) - \mu, \quad (25)$$

$$\omega(k) = \left[[(1-\delta)^2 - \phi^2](1-2\chi) - \frac{2t}{J}\phi\right](2J)\cos(k), \quad (26)$$

while the self-consistent equations for the order parameters χ and ϕ can be obtained by minimizing the free energy. We can now proceed to a brief discussion of the results in the MFA.

B. Ground-state properties at half-filling

At half-filling, there are no charge degrees of freedom, and the t-J model (24) reduces to the antiferromagnetic Heisenberg model in the fermion representation,

$$H_J = \sum_k \omega_0(k) f_k^\dagger f_k + 2NJ\chi^2. \quad (27)$$

In this case the order parameter χ can be evaluated to be $\chi = -1/\pi$, and we obtain a gapless spinon spectrum,

$$\omega_0(k) = \left(1 + \frac{2}{\pi}\right)(2J)\cos(k), \quad (28)$$

which is rather close to the exact result of the Heisenberg chain obtained by using the Bethe-ansatz method,[35] $\omega_0(k) = (\pi/2)(2J)\cos(k)$. Correspondingly, the spinon spectrum near the spinon Fermi surface ($k = \pm\pi/2$) is linear with velocity $v_s = (1 + 2/\pi)(2J) = 1.6366(2J)$, which is also very close to the exact result of the Heisenberg chain obtained by Haldane,[36] $v_s = (\pi/2)(2J) = 1.5708(2J)$. The ground state energy of the Heisenberg model at temperature $T = 0$ is $E_0 = -0.4196(2J)$ which is only 5.3% higher than the exact Bethe-ansatz value[35] of $E_0 = -(1/4 - \ln 2)(2J) = -0.4431(2J)$.

Thus in the half-filled case, the spinon has a gapless spectrum, and the spinon ground state energy can be described adequately by the Jordan-Wigner transformation within the MFA. This case has already been considered earlier.[29,37]

C. Ground-state energy away from half-filling

Away from half-filling, a gapless holon spectrum is obtained

$$\varepsilon(k) = -2t\frac{2}{\pi}\cos(k), \quad (29)$$

from which the holon Fermi velocity is given by

$$v_h = 2t\frac{2}{\pi}\sin[(1-\delta)\pi] = 2t\frac{2}{\pi}\sin(\delta\pi), \tag{30}$$

and the holon ground state energy at temperature $T = 0$ is obtained as

$$E_h = -\left(\frac{2t}{\pi}\right)\left(\frac{2}{\pi}\right)\sin(\delta\pi). \tag{31}$$

All these quantities differ from the corresponding exact values[5] of the 1D large-U limit Hubbard model $\varepsilon(k) = -2t\cos(k)$, $v_h = 2t\sin(\delta\pi)$, and $E_h = -(\frac{2t}{\pi})\sin(\delta\pi)$, only by a factor $2/\pi$.

At the same time, the gapless spinon spectrum at finite dopings becomes

$$\omega(k) = \left[\left((1-\delta)^2 - \frac{\sin^2(\delta\pi)}{\pi^2}\right)\left(1+\frac{2}{\pi}\right) + \frac{2t}{J}\frac{1}{\pi}\sin(\delta\pi)\right](2J)\cos(k), \tag{32}$$

with the spinon ground state energy

$$E_s = -(1-\delta)^2\left[1 - \frac{\sin^2(\delta\pi)}{\pi^2(1-\delta)^2}\right]E_0, \tag{33}$$

which is again very close to the exact result of the spinon ground state energy[5] of the 1D large-U limit Hubbard model over the entire doping range. Here E_0 is the ground state energy at half-filling. Therefore the total ground state energy of the 1D t-J model in the fermion-spin approach within the MFA can be expressed as

$$\begin{aligned} E_g &= E_h + E_s \\ &= -\left(\frac{2t}{\pi}\right)\left(\frac{2}{\pi}\right)\sin(\delta\pi) \\ &\quad -(1-\delta)^2\left[1 - \frac{\sin^2(\delta\pi)}{\pi^2(1-\delta)^2}\right]0.4196(2J). \end{aligned} \tag{34}$$

The ground state energy and thermodynamical quantities for the 1D Hubbard model in the atomic limit were calculated a long time ago.[38] Our result for the ground state energy is rather close to theirs.

D. Momentum distribution

Now we turn to discuss the global features of the electron-momentum distribution within the MFA. This distribution for the physical electron is defined as

$$n(k) = \sum_\sigma \langle \tilde{C}^\dagger_{k\sigma}\tilde{C}_{k\sigma}\rangle = \frac{1}{N}\sum_{lm\sigma} e^{ik(x_l - x_m)}\langle \tilde{C}^\dagger_{l\sigma}\tilde{C}_{m\sigma}\rangle. \tag{35}$$

In the present fermion-spin approach, neglecting the effects due to the projection operator defined in Sec. II C, this distribution function can be rewritten as

$$n(k) = \frac{1}{N}\sum_{lm} e^{ik(x_l - x_m)}\langle a^\dagger_l a_m (S^+_l S^-_m + S^-_l S^+_m)\rangle. \tag{36}$$

Using the Jordan-Wigner transformation (16)–(18), $n(k)$ can be further expressed as

$$n(k) = \frac{1}{N}\sum_{lm} e^{ik(x_l - x_m)}\langle a^\dagger_l a_m (f^\dagger_l e^{i\pi(\sum_{i<l} f^\dagger_i f_i - \sum_{j<m} f^\dagger_j f_j)} f_m + f_l e^{-i\pi(\sum_{i<l} f^\dagger_i f_i - \sum_{j<m} f^\dagger_j f_j)} f^\dagger_m)\rangle. \tag{37}$$

Since $e^{\pm i\pi f^\dagger_i f_i} = 1 - 2f^\dagger_i f_i$, in the MFA, we obtain

$$n(k) = 1 - \delta + \sum_{m=1}^{\infty}(-1)^{m+1}\left(\frac{2}{\pi}\right)^{m+1}\frac{\sin(m\delta\pi)}{m}\cos(mk), \tag{38}$$

which is plotted (solid line) in Fig. 1 for doping $\delta = 0.5$. For comparison, the corresponding curves for the slave-boson (dashed line) and the slave-fermion (dot-dashed line) cases are also given. It is obvious that $n_k \geq 1-\delta$ in the slave-boson case and $\leq 1-\delta$ in the slave-fermion case, which is very far from a should-be electron-momentum distribution. The integrated area under the curve is equal to $(1-\delta^2)$ in the slave-boson case and is $(1-\delta)^2$ in the slave-fermion case, while the correct value should be $1-\delta$.[24] The solid curve corresponding to our transformation is closer to the exact result.[5] The integrated area is correct and the shape looks like a reasonable momentum distribution, i.e., in some part the distribution is greater, while in the other part it is less than $1-\delta$. To get a more accurate result (including the correct location of the Fermi surface and a correct slope at it) one should go beyond the MFA to include the spinon-holon interactions as discussed in the next section.

Thus away from half-filling, the spinons and holons are decoupled completely, with the holon behaving like a spinless fermion, while the spinon has the Jordan-Wigner[25] form in 1D. The gapless spectra for both holons

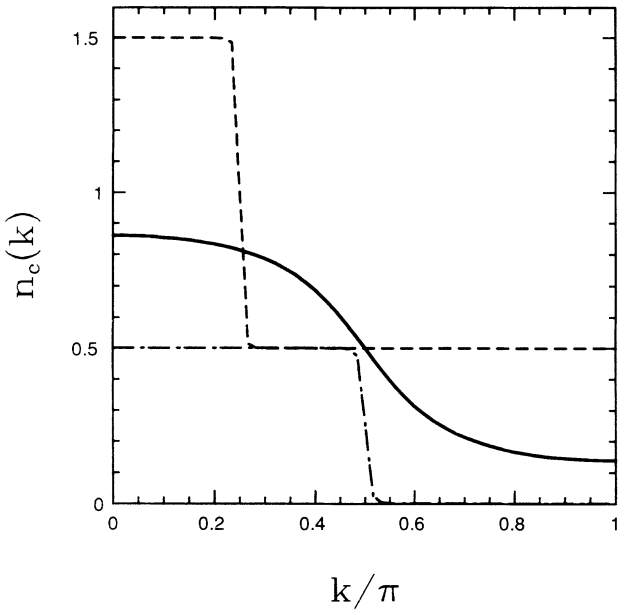

FIG. 1. The momentum distribution of physical electrons in the mean-field approximation obtained by the fermion-spin transformation proposed in this paper (solid line) in comparison with corresponding curves in the slave-boson (dashed line) and the slave-fermion (dot-dashed line) approaches. The doping concentration $\delta = 0.5$.

and spinons, as well as the ground state energy, can be described adequately within the fermion-spin approach even in the MFA.

IV. THE ASYMPTOTIC BEHAVIOR OF CORRELATION FUNCTIONS IN THE 1D CASE

A. Motivation

Interacting 1D electron systems generally behave like Luttinger liquids[12] where the electron correlation functions show a power-law decay with unusual exponents. These systems exhibit an electron Fermi surface with a correct Luttinger volume but the momentum distribution function is singular at the Fermi surface, also with unusual exponents.[5]. These exponents depend on the interaction strength. Haldane[12] has shown that the characteristics of Luttinger liquids can be calculated using the bosonization techniques. To get more insight into the problem let us consider the Bethe ansatz wave function for the Hubbard model in the large-U limit (hence for the t-J model in the small-J limit), derived by Ogata and Shiba,[5]

$$\Psi(x_1,...,x_N) = \det[\exp(ik_i x_{Q_i})]\Phi(y_1,...,y_M), \quad (39)$$

where the determinant depends only on the coordinates x_{Q_j} of particles, but not on their spins, while $\Phi(y_1,...,y_M)$ is the Bethe ansatz wave function for an AF Heisenberg chain with $y_1,\ldots,y_M$ as coordinates of down spins.[35] This asymptotic form can be interpreted as a complete separation of charge and spin degrees of freedom in some sense. In fact, the determinant describes spinless fermions (holons), whereas Φ is the "spinon" wave function. Our fermion-spin transformation is, to some extent, an approximate second quantized version of this solution, with the holon being represented by a spinless fermion and the spin represented by a *hard-core* boson.

However, there is an important "detail" in the wave function (39), namely, the spin wave function Φ is for a "*squeezed*" Heisenberg chain, i.e., all holes should be removed. This will lead to rearrangement of spin configurations and far-reaching nonlocal effects. Therefore, spinons and holons are not completely independent, but interacting with each other rather strongly. As shown in Ref. 5, the correct exponents of correlation functions and an adequate description of the momentum distribution function (Fermi surface at k_F, rather than $2k_F$ with appropriate singular behavior) can be obtained only if these interaction effects are properly taken into account. Weng *et al.*[29] have shown that the effects due to squeezing and rearrangement of spin configurations can be included by introducing a nonlocal "string" field. After doing that correct results for the correlation function exponents, etc., can be obtained for a 1D t-J chain. In this section we calculate these exponents within our fermion-spin approach, following their technique with some modifications. The nonlocal effects due to spinon-holon and spinon-spinon interactions will be included by introducing two string fields. After squeezing, there are no holes in the chain, so the additional degrees of freedom due to assigning "spin" to a hole site disappear, hence the projection operator introduced in Sec. II C is not needed for our purpose.

B. String operators

Let us consider the t-term in the t-J Hamiltonian within the fermion-spin representation. Following Ref. 29, the largest holon kinetic energy may be obtained if the spin configurations are squeezed as

$$P_i(a_i^\dagger S_i^+ P_i^\dagger P_{i+1} a_{i+1} S_{i+1}^- + a_i^\dagger S_i^- P_i^\dagger P_{i+1} a_{i+1} S_{i+1}^+) P_{i+1}^\dagger = a_i^\dagger a_{i+1} \quad (40)$$

for all sites i where a holon is present. However, after such squeezing, the spin configurations are not optimal to favor the spinon energy. Thus at the same time spin configurations must be rearranged into optimum configurations to provide the lowest spinon energy. These optimum spin configurations can be obtained by reversing the original spin polarization for all sites on the left-hand side of site i. These processes of first squeezing the t-J chain and then rearranging the spin configurations, are shown schematically in Fig. 2. These nonlocal processes cannot be described by any formal perturbation theory, but can be taken into account approximately by introducing the string fields.[29,24] In our case, we introduce two string fields to describe the above physical processes, so

the constrained electron operator $\tilde{C}_{i\sigma}$ can be expressed within the fermion-spin approach as

$$\tilde{C}_{i\uparrow} = (e^{i\pi(N-\sum_{l>i} a_l^\dagger a_l)} a_i)(e^{-i\pi\sum_{l<i} a_l^\dagger a_l} S_i^-), \quad (41)$$

$$\tilde{C}_{i\downarrow} = (e^{i\pi(N+\sum_{l>i} a_l^\dagger a_l)} a_i)(e^{i\pi\sum_{l<i} a_l^\dagger a_l} S_i^+), \quad (42)$$

which means that the spinless fermion a_i and the hard-core boson $S_i^\pm$ are replaced by corresponding string operators as

$$a_i \to a_i e^{i\pi(N\pm\sum_{l>i} a_l^\dagger a_l)}, \quad (43)$$

$$S_i^\pm \to S_i^\pm e^{\pm i\pi\sum_{l<i} a_l^\dagger a_l}, \quad (44)$$

where $e^{\pm i\pi\sum_{l<i} a_l^\dagger a_l}$ is the string field for the spinon due to the presence of holons, describing the effects of rearrangements of spin configurations from $-\infty$ to site i when an electron is removed or added at site i. For the t-J chain, holons on the right-hand side of site i can feel some indirect effects of holons on the left-hand side of site i due to the rearrangements of spin configurations from $-\infty$ to site i when one electron was removed or added at site i. These indirect effects can be described by the string field $e^{i\pi(N\pm\sum_{l>i} a_l^\dagger a_l)}$ for the holon. One can check easily that the anticommutation relations for the physical electron are preserved exactly in our case.

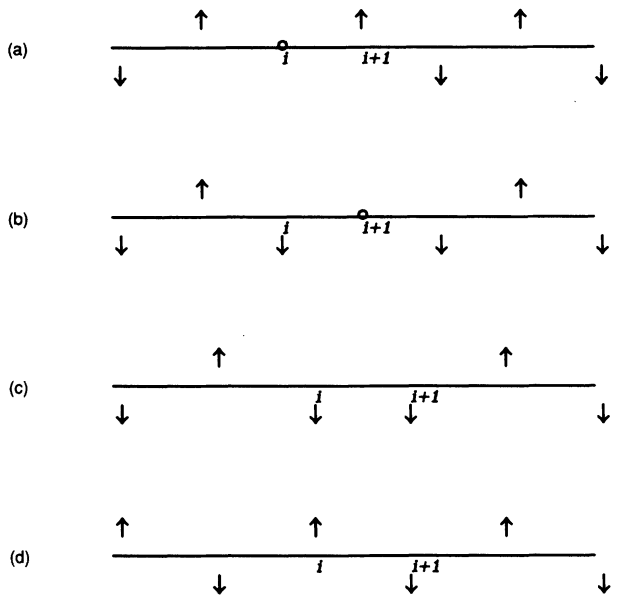

FIG. 2. The spin background is assumed to be an antiferromagnetic state for the $J > 0$ case of the 1D t-J model. The t-J chain is squeezed and the spin configuration is rearranged due to the spin-up electron hopping: (a) Before hopping, when the holon is at site i. (b) After hopping, when the holon has hopped to site $i+1$ from site i, while the spinon has hopped to site i from site $i+1$. The spin polarization directions to the left of the hole are already optimized by the fermion-spin transformation, but there is still a hole in the chain. (c) Squeezing out the hole from the t-J chain. After this squeezing, the spin configuration is not optimal to favor the lowest spinon energy. (d) Rearranging the spin configuration from $-\infty$ to site i to favor the lowest spinon energy. The situation for the spin-down electron hopping is similar.

C. Energy spectrum for a squeezed chain

After *squeezing* and rearranging the spin configurations, the t-J model can be written as

$$H = -t\sum_i (a_i^\dagger a_{i+1} + \text{H.c.}) - \mu\sum_i a_i^\dagger a_i + J[(1-\delta)^2 - \phi^2]\sum_{\langle ij\rangle} \mathbf{S}_i \cdot \mathbf{S}_j, \quad (45)$$

where we have approximated the probability of the spin exchange process of the Heisenberg term as $a_i^\dagger a_i a_j^\dagger a_j \approx \langle a_i^\dagger a_i\rangle\langle a_j^\dagger a_j\rangle - \langle a_i^\dagger a_j\rangle\langle a_j^\dagger a_i\rangle = (1-\delta)^2 - \phi^2$, and the lattice constant of the squeezed spin chain has become $a/(1-\delta)$, where a is the original lattice constant. Therefore the Fermi points of spinons are shifted from $k_F = \pm\pi/2$ of the half-filled case to $k_F = \pm\pi(1-\delta)/2$ for the doped case.

For the *squeezed* chain, the gapless holon spectrum, the holon Fermi velocity, and the holon ground state energy are

$$\varepsilon(k) = -2t\cos(k), \quad (46)$$

$$v_h = 2t\sin(\delta\pi), \quad (47)$$

$$E_t = -\frac{2t}{\pi}\sin(\delta\pi), \quad (48)$$

respectively, which are in full agreement with the corresponding exact values of the 1D large-U Hubbard model.[5] At the same time, the gapless spinon spectrum, spinon Fermi velocity, and the spinon ground state energy are given by

$$\omega(k) = \left[(1-\delta)^2 - \frac{\sin^2(\delta\pi)}{\pi^2}\right](2J)\cos(k), \quad (49)$$

$$v_s = [(1-\delta)^2 - \sin^2(\delta\pi)/\pi^2](2J)\cos(\delta\pi/2), \quad (50)$$

$$E_J = \left[(1-\delta)^2 - \frac{\sin^2(\delta\pi)}{\pi^2}\right]E_0, \quad (51)$$

respectively, which are very close to the corresponding exact values of the 1D large-U limit Hubbard model.[5] Here E_0 is the ground state energy at half-filling. Therefore, the total energy of the t-J model $E_g = E_t + E_J$ agrees quantitatively with the exact value of the 1D large-U limit Hubbard model in the entire doping range. It fully agrees with the 1D results for the Hubbard model obtained earlier in the atomic limit.[38] The gapless spinon and holon spectra and the ground state energy are all better than the mean-field results obtained in Sec. III, which indicates that the string fields take into account the spinon-holon interactions in the t-J model, and renormalize considerably the results obtained in the MFA without string fields.

D. Correlation functions

The spin-spin correlation function is defined as

$$\begin{aligned} S(x_i - x_j, t) &= \langle S_i^X(t) S_j^X(0)\rangle = \langle S_i^Y(t) S_j^Y(0)\rangle \\ &= \langle S_i^Z(t) S_j^Z(0)\rangle \\ &= \frac{1}{4}\langle S_i^+(t) S_j^-(0) + S_i^-(t) S_j^+(0)\rangle. \end{aligned} \tag{52}$$

In the doped case, we need to replace the operator $S_i^{\pm}$ in Eq. (52) by Eq. (44) to account for the presence of holons. Thus substituting Eq. (44) into Eq. (52), we obtain the spin-spin correlation function of the t-J model as

$$\begin{aligned} S(x_i - x_j, t) = \frac{1}{4}[&\langle S_i^+(t) S_j^-(0)\rangle \langle e^{i\pi \sum_{l<i} a_l^\dagger(t) a_l(t)} e^{-i\pi \sum_{l<j} a_l^\dagger(0) a_l(0)}\rangle \\ &+ \langle S_i^-(t) S_j^+(0)\rangle \langle e^{-i\pi \sum_{l<i} a_l^\dagger(t) a_l(t)} e^{i\pi \sum_{l<j} a_l^\dagger(0) a_l(0)}\rangle]. \end{aligned} \tag{53}$$

Following Haldane,[12,29] we apply the bosonization method to the free holon field, and obtain the following asymptotic form:

$$\langle e^{\pm i\pi \sum_{l<i} a_l^\dagger(t) a_l(t)} e^{\mp i\pi \sum_{l<j} a_l^\dagger(0) a_l(0)}\rangle \sim \frac{1}{[(x_i - x_j)^2 - (v_h t)^2]^{\frac{1}{4}}}, \tag{54}$$

where v_h is the holon Fermi velocity. Luther and Peschel[34] have mapped the 1D Heisenberg model into an interacting spinless fermion system by using the Jordan-Wigner[25] transformation. Their work involves generalization of the Jordan-Wigner transformation to provide a representation for continuum spin operators. The asymptotic form of the spin-spin correlation function of the Heisenberg model can then be obtained by considering the spinon-spinon interactions. Following their calculation, we get

$$\langle S_i^+(t) S_j^-(0) + S_i^-(t) S_j^+(0)\rangle \sim \frac{\cos[2k_F(x_i - x_j)]}{[(x_i - x_j)^2 - (v_s t)^2]^{\frac{1}{2}}}, \tag{55}$$

where v_s is the spinon Fermi velocity. Combining Eq. (54) with Eq. (55), we obtain the asymptotic form of the spin-spin correlation function of the 1D t-J model as

$$\begin{aligned} S(x_i - x_j, t) \sim &\frac{1}{[(x_i - x_j)^2 - (v_h t)^2]^{\frac{1}{4}}} \\ &\times \frac{\cos[2k_F(x_i - x_j)]}{[(x_i - x_j)^2 - (v_s t)^2]^{\frac{1}{2}}}, \end{aligned} \tag{56}$$

which shows a power-law decay with exponent 3/2, in full agreememt with the numerical result of the 1D large-U limit Hubbard model obtained by Ogata and Shiba.[5]

E. Momentum distribution function

The electron-momentum distribution function $n(k)$ is defined in Eq. (36) within the fermion-spin approach. To consider the *squeezing* effect and rearrangements of the spin configurations, we need to substitute Eqs. (43) and (44) into Eq. (36). Then $n(k)$ can be rewritten as

$$n(k) = \frac{2}{N}\sum_{ij} e^{ik(x_i - x_j)} \langle e^{i\frac{\pi}{2}\sum_{l<i} a_l^\dagger a_l} a_i^\dagger S_i^+ G_i^* G_j S_j^- a_j e^{-i\frac{\pi}{2}\sum_{l<j} a_l^\dagger a_l}\rangle, \tag{57}$$

where the factor $G_i = e^{i\frac{\pi}{2}(N - \sum_{l>i} a_l^\dagger a_l)}$. In what follows, we will drop this factor as in the previous calculations,[29,24] since it will only contribute a next-to-leading additional power-law decay in the asymptotic single-electron Green's function, so one may neglect it if only interested in the leading contribution.

The calculation for the global features of $n(k)$ is similar to the case without string fields within the MFA and the result is

$$\begin{aligned} n(k) &= 1 - \delta + A_1(k) + A_2(k) + A_3(k) + \cdots, \\ A_1(k) &= \left(\frac{2}{\pi}\right)^2 \sin(\delta\pi)\cos(k), \end{aligned}$$

$$A_2(k) = \left(\frac{2}{\pi}\right)^3 \left[\frac{1}{\pi}\sin^2(\delta\pi) - \frac{\delta}{2}\sin(2\delta\pi)\right]\cos(2k),$$

$$A_3(k) = \left(\frac{2}{\pi}\right)^4 \left[\frac{1}{\pi}\sin(\delta\pi)\sin(2\delta\pi) + \frac{1}{3}\left(1 - \frac{2\delta}{3}\right)\sin(3\delta\pi)\right]\cos(3k). \quad (58)$$

The curve $n(k)$ is plotted in Fig. 3 (solid line) for $\delta = 0.25$ in comparison with the result without string fields (dot-dashed line). We find some substantial improvement by including the string fields. In particular, the location of the Fermi points was wrong in the MFA without string fields, while it is correct $[k_F = \frac{\pi}{2}(1-\delta)]$ if they are included. In the same figure we have also plotted the $n(k)$ curve obtained in the early treatment (dashed line)[24] for the CP^1 electron representation (without accounting for the *hard-core* nature of the bosons). Obviously, the global features of this curve are not correct [$n(k)$ goes up again as k further increases]. Nevertheless, the asymptotic form of the momentum distribution near k_F, obtained in both approaches, is correct, namely,

$$n(k) \sim \text{const} - C|k - k_F|^{\frac{1}{8}}\text{sgn}(k - k_F), \quad (59)$$

again in agreement with the exact numerical result.[5] This singularity is washed out in the numerical calculations and does not show up in Fig. 3.

To sum up we have confirmed that by introducing the string fields the spinon-holon interactions can be included to some extent, which allows us to obtain correct exponents for the correlation functions and momentum distribution, as proposed earlier.[29] Moreover, the global features of the energy spectrum and the momentum distribution, found in our fermion-spin approach, are correct in contrast with the previous approach,[29] which could not provide such an adequate description.

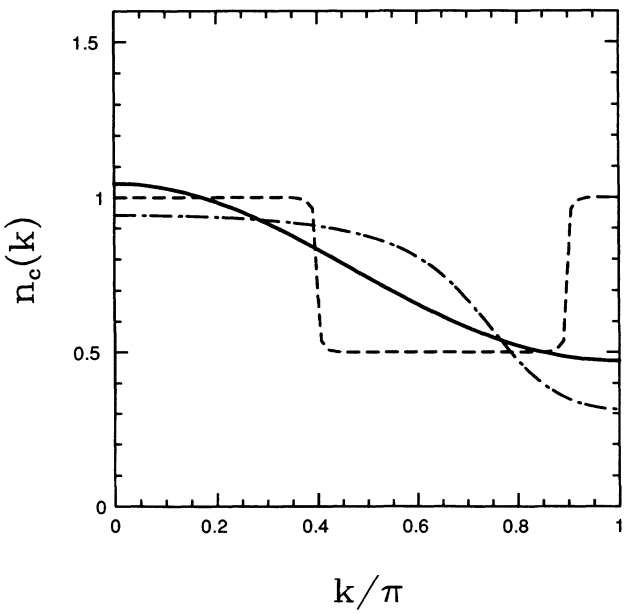

FIG. 3. The momentum distribution of physical electrons in the mean-field approximation obtained by the fermion-spin transformation with the string fields (solid line), and without string fields (dot-dashed line), in comparison with the corresponding curve in the conventional CP^1 approach (dashed line) (see Ref. 24). The doping concentration $\delta = 0.25$.

V. THE MEAN-FIELD THEORY IN 2D WITHIN THE FERMION-SPIN APPROACH

In this section, we consider the 2D t-J model. Very soon after the discovery of oxide superconductors Anderson[1] revived his idea of the resonating valence bond (RVB) to describe the short-range AF fluctuations in the 2D Hubbard model. Baskaran, Zou, and Anderson[39] developed a mean-field theory of the RVB state. Later a number of other more elaborate mean-field solutions were discussed both at half-filling and away from it, such as the flux phase,[40] the spiral phase,[41,23] and the commensurate flux phase,[42] which breaks the time-reversal symmetry and parity. The latter is related to the proposed fractional statistics and anyon superconductivity.[43] For the early suggested flux phase,[40] the lowest energy solution is a state with $\frac{1}{2}$ flux quantum (or phase π) per plaquette, which does not break the time-reversal symmetry and parity. Sheng, Su, and Yu found that the π-flux phase can coexist with the $s + id$ wave RVB state for small dopings.[44] Lee and Feng,[22] and later Chen, Su, and Yu[45] found that the magnetized RVB state with coexisting AF order and a d-wave RVB order parameter has a gain in energy. Furthermore, Hsu[46] has shown that the magnetized flux state which is the coexistence of AF order with a flux state has a similar gain in energy. Recently, Wang[37] and Ubbens and Lee[47] obtained the same result in a different framework. In this section, we discuss the 2D t-J model along this line.

A. Generalized Jordan-Wigner transformation

In the fermion-spin approach, the success of the theory depends strongly on whether one can map the *hard-core boson* onto an appropriate fermion or boson representation. In the 2D case, the Jordan-Wigner transformation of the spin operators has been generalized by several authors.[26] In particular, Wang[37] discussed the Heisenberg model in the MFA using this generalized Jordan-Wigner transformation. Using our fermion-spin transformation (7), this mean-field calculation can be easily generalized to the t-J model. The generalized Jordan-Wigner transformation may be written as[26,37]

$$S_i^+ = f_i^\dagger e^{i\theta_i}, \quad (60)$$

$$S_i^- = f_i e^{-i\theta_i}, \quad (61)$$

$$S_i^Z = f_i^\dagger f_i - \frac{1}{2}, \quad (62)$$

where f_i is a spinless fermion, $\theta_i = \sum_{l\neq i} f_l^\dagger f_l B_{il}$. In order to preserve the *hard-core* properties of the spin op-

erators, B_{il} should be such that $e^{iB_{il}} = -e^{iB_{li}}$. One possible way of materializing this equality is to set $B_{il} = \mathrm{Im}\ln(Z_l - Z_i)$, with a complex representation of the lattice sites $Z_l = X_l + iY_l$. If the effects connected with the projection operator P are neglected, then the 2D t-J model can be mapped onto the fermion representation as

$$H = -t\sum_{\langle ij\rangle} h_i h_j^\dagger (f_i^\dagger f_j e^{i(\theta_i-\theta_j)} + \mathrm{H.c.}) - \mu\sum_i h_i h_i^\dagger + J\sum_{\langle ij\rangle} h_i h_i^\dagger h_j h_j^\dagger [\tfrac{1}{2}(f_i^\dagger f_j e^{i(\theta_i-\theta_j)} + \mathrm{H.c.}) + (f_i^\dagger f_i - \tfrac{1}{2})(f_j^\dagger f_j - \tfrac{1}{2})]. \quad (63)$$

It has been shown[26,37] that the phase factor in the Hamiltonian (63) creates a gauge field, with the vector potential given by

$$\mathbf{A}(r_i) = \sum_{l\neq i} n_l \frac{\hat{z}\times(r_l - r_i)}{(r_l - r_i)^2}, \quad (64)$$

where $n_l = f_l^\dagger f_l$. On average, there is a π-flux attached to each spinless fermion f_i, which is nothing but the Chern-Simons gauge field converting a *hard-core boson* into a spinless fermion. As mentioned earlier, the π-flux does not break the time-reversal symmetry and parity.

The Hamiltonian (63) is obviously very complicated, so a more complete discussion about it beyond the MFA will be given elsewhere. In this section, we only discuss some mean-field properties of the 2D t-J model within the fermion-spin approach. In the MFA, following the similar discussion of Laughlin *et al.*,[43] Mele,[26] and Wang,[37] the phase factor is absorbed by redefining a bond-dependent exchange parameter J_{ij}. At half-filling, there are many possible phases and the state with the lowest energy[37] turned out to be the magnetized flux state with a coexisting Néel order parameter $\langle S_i^Z\rangle = (-1)^i M$ and an orbital current order parameter $\langle S_i^+ S_{i+\nu}^-\rangle = \chi$, where $\nu = \pm x, \pm y$. The ground state energy per bond is $E_0 = -0.33J$, while the staggered magnetization is $M = 0.389$, which are rather close to the best numerical estimates[48] $E_0 = -0.3346J$ and $M = 0.31$, respectively. This state is completely equivalent to what was first discussed by Hsu,[46] who obtained the ground state energy $E_0 = -0.331J$ and staggered magnetization $M \approx 0.3$ within a different theoretical framework. All these results show the accuracy of the mean-field result within the generalized Jordan-Wigner transformation.[26]

B. Mean-field theory away from half-filling

Away from half-filling we need to introduce an additional holon particle-hole order parameter $\phi = \langle h_i^\dagger h_{i+\nu}\rangle$, and the t-J model can be decoupled in the MFA as

$$H = 2t\chi\sum_{\langle jl\rangle} h_j^\dagger h_l - \mu\sum_j h_j h_j^\dagger + (J_{\mathrm{eff}} + 2t\phi - 2J_{\mathrm{eff}}\chi)\sum_{\langle jl\rangle} e^{i(\theta_j-\theta_l)} f_j^\dagger f_l - 2J_{\mathrm{eff}}M\sum_{\langle jl\rangle}(-1)^l f_j^\dagger f_j + 4NJ_{\mathrm{eff}}\chi^2 - 8Nt\chi\phi + 4NJ_{\mathrm{eff}}M^2, \quad (65)$$

where $J_{\mathrm{eff}} = J[(1-\delta)^2 - \phi^2]$, and N is the number of lattice sites. In the magnetized flux phase, the t-J model can be diagonalized by using the Bogoliubov transformation to give

$$H = \sum_{k(\mathrm{red})} (\varepsilon_k^- \alpha_k^\dagger \alpha_k + \varepsilon_k^+ \beta_k^\dagger \beta_k) + \sum_{k(\mathrm{red})} (E_k A_k^\dagger A_k - E_k B_k^\dagger B_k) + 4NJ_{\mathrm{eff}}\chi^2 - 8Nt\chi\phi + 4NJ_{\mathrm{eff}}M^2, \quad (66)$$

where (red) means the summation is carried only over the reduced Brillouin zone. The new operators α_k, β_k, A_k, and B_k are related to h_k^A, h_k^B, f_k^A, and f_k^B by

$$h_k^A = \frac{1}{\sqrt{2}}(\alpha_k + \beta_k), \qquad h_k^B = \frac{1}{\sqrt{2}}(\alpha_k - \beta_k), \quad (67)$$

and

$$f_k^A = \frac{\cos k_y - i\sin k_x}{\sqrt{\cos^2 k_y + \sin^2 k_x}}(u_k A_k - v_k B_k), \qquad f_k^B = u_k B_k + v_k A_k, \quad (68)$$

where

$$u_k^2 = \frac{1}{2}\left(1 + \frac{8JM}{E_k}\right), \qquad v_k^2 = \frac{1}{2}\left(1 - \frac{8JM}{E_k}\right), \quad (69)$$

and the spin excitation spectrum is

$$E_k = \sqrt{(8J_{\mathrm{eff}}M)^2 + 4(J_{\mathrm{eff}} + 2t\phi - 2J_{\mathrm{eff}}\chi)^2(\cos^2 k_y + \sin^2 k_x)}, \quad (70)$$

while the charge excitation spectrum is

$$\epsilon_k^{\pm} = \pm 2t\chi\gamma_k - \mu, \quad \gamma_k = 2(\cos k_x + \cos k_y). \tag{71}$$

In obtaining the above results, we have considered two sublattices A and B with $i \in A$ and $i+\nu \in B$. The free energy of the 2D t-J model can be obtained as

$$\begin{aligned} F = &-\frac{1}{\beta}\sum_{k(\mathrm{red})} \ln[(1+e^{-\beta\epsilon_k^-})(1+e^{-\beta\epsilon_k^+})] \\ &-\frac{1}{\beta}\sum_{k(\mathrm{red})} \ln[(1+e^{-\beta E_k})(1+e^{\beta E_k})] \\ &+4NJ_{\mathrm{eff}}\chi^2 - 8Nt\chi\phi + 4J_{\mathrm{eff}}M^2, \end{aligned} \tag{72}$$

from which we find the self-consistent equations for the order parameters χ, M, ϕ by minimizing the free energy with respect to these parameters.

C. Doping dependence of the staggered magnetization

At half-filling, the 2D t-J model reduces to a 2D AF Heisenberg Hamiltonian, and the result is the same as discussed by Hsu[46] and Wang.[37] The spinon spectrum in the magnetized flux phase with AF long-range order is expressed as

$$E_k = \sqrt{(8JM)^2 + 4J^2(1-2\chi)^2(\cos^2 k_y + \sin^2 k_x)}, \tag{73}$$

where a gap appears due to the presence of AF staggered magnetization. We note that a gap in the spinon spectrum of the flux phase at half-filling was suggested by Laughlin earlier.[43] However, this gap coming from the staggered magnetization M decreases very rapidly upon doping. In the MFA, M vanishes around doping $\delta \approx 0.1 - 0.15$ for $t/J = 3-5$, which is plotted in Fig. 4(a). This result is in reasonably good agreement with experiments[49,50] and Monte-Carlo simulations.[22] For comparison we note that the magnetization vanishes only at $\delta \approx 0.62$ in the MFA for the slave-fermion approach.[23] At finite dopings, but still within the magnetized flux phase, we find a competition between the Néel order parameter M and the orbital current order parameter χ, with M decreasing very rapidly [see Fig. 4(a)], and $-\chi$ increasing very fast [see Fig. 4(b)] upon doping. In the small doping range, the holon particle-hole order parameter ϕ increases roughly linearly upon doping, and is almost independent of t/J, which is shown in Fig. 4(c). The t-J model is characterized by a competition between the kinetic energy (t) and the magnetic energy (J). The magnetic energy J favors an AFLRO for the spins, whereas the kinetic energy t favors delocalization of the holes and tends to destroy the spin AFLRO. Thus the rapid suppression of the AFLRO upon doping means that the present mean-field kinetic energy is better than those obtained in the slave-fermion approach and is closer to the optimal kinetic energy of the system. Beyond doping $\delta \approx 0.1 - 0.15$, corresponding to the range of the actual high-temperature superconductors, there is no AFLRO, but short-range AF correlations persist and the spinons are in a disordered flux phase with a gapless spectrum,

$$E_k = 2(J_{\mathrm{eff}} + 2t\phi - 2J_{\mathrm{eff}}\chi)\sqrt{\cos^2 k_y + \sin^2 k_x}, \tag{74}$$

as conjectured by Anderson.[1] This spinon spectrum is similar to that of the flux state discussed also at the mean-field level by Affleck and Marston and Kotliar.[40]

The mean-field phase boundary between the magnetized flux and disordered flux states is, of course, at somewhat higher doping δ than the value given by experiments and numerical simulations. In fact, the frustrations of spins can shift the mean-field phase boundary towards smaller doping δ.[51] Thus we believe that the result will be even closer to experiments and numerical simulations by going beyond the MFA.

D. Specific heat

The specific heat measurements on oxide superconductors have been made for many compounds by different researchers.[52] The descrepancies are mostly due to the difficulty in preparing and characterizing samples of the oxide compounds. Although the specific heat data for the superconducting compounds show considerable variations for samples measured by different groups, some qualitative features seem common to all the measurements. Hence a quantitative comparison between theory and experiment is still early, but the qualitative tendency of the specific heat in an adequate theoretical description should be consistent with experiments.

In the half-filled case, there are no charge degrees of freedom and the spinon specific heat has been considered by Wang.[37] Away from half-filling, we are interested in the doping range $\delta = 0.1-0.2$ where the superconductivity appears. In this doping range, we have shown that the magnetization M vanishes and the system is in a disordered flux state, where the internal energy of the system in the MFA is given by

$$U(T) = 4NJ_{\mathrm{eff}}\chi(1-\chi^2) - 8Nt\chi\phi, \tag{75}$$

from which the specific heat can be obtained as

$$C_v(T) = \left(\frac{\partial U}{\partial T}\right)_V. \tag{76}$$

The numerical result is shown in Fig. 5 at doping $\delta = 0.2$ for t/J=3 (solid line), t/J=5 (dashed line), and the shape is similar to the experimental results.[52,53] For $T > 0.0005J$, the specific heat is found to increase with temperature T, which is also consistent with the experiments. Therefore our simple mean-field calculation provides a correct qualitative description of the specific heat for oxide compounds.

E. Phase separation

The possible phase separation in the t-J model was proposed by Emery, Kivelson, and Lin.[54] They argued that the dilute holes in an antiferromagnet are unsta-

ble against phase separation into hole-rich and no-hole phases, and the transition from an ordered state to a doped state is of first order. Later investigation[55] using high-temperature expansions shows that a line of the phase separation extends from $J/t = 3.8$ at zero filling to $J/t = 1.2$ near half-filling, but for the range of parameter interesting to the copper oxide planes there is no evidence for phase separation. Within the mean-field theory of our fermion-spin approach, we find that the phase separation is robust for the t-J model, and the phase separation manifests itself at the mean-field level by a negative compressibility (slope of the chemical potential). The total energy $E_{\rm total}$ and the chemical potential μ as a function of the doping δ for $t/J = 5$ is plotted in Fig. 6, which shows that the phase separation occurs roughly at dopings $\delta \leq \delta_c = 0.08$. In this doping range ($\delta \leq \delta_c$), the compressibility of the t-J model is negative, and therefore the magnetized flux state with long-range order is unstable. The range of the phase separation will be reduced by considering the frustrations of spins.[51]

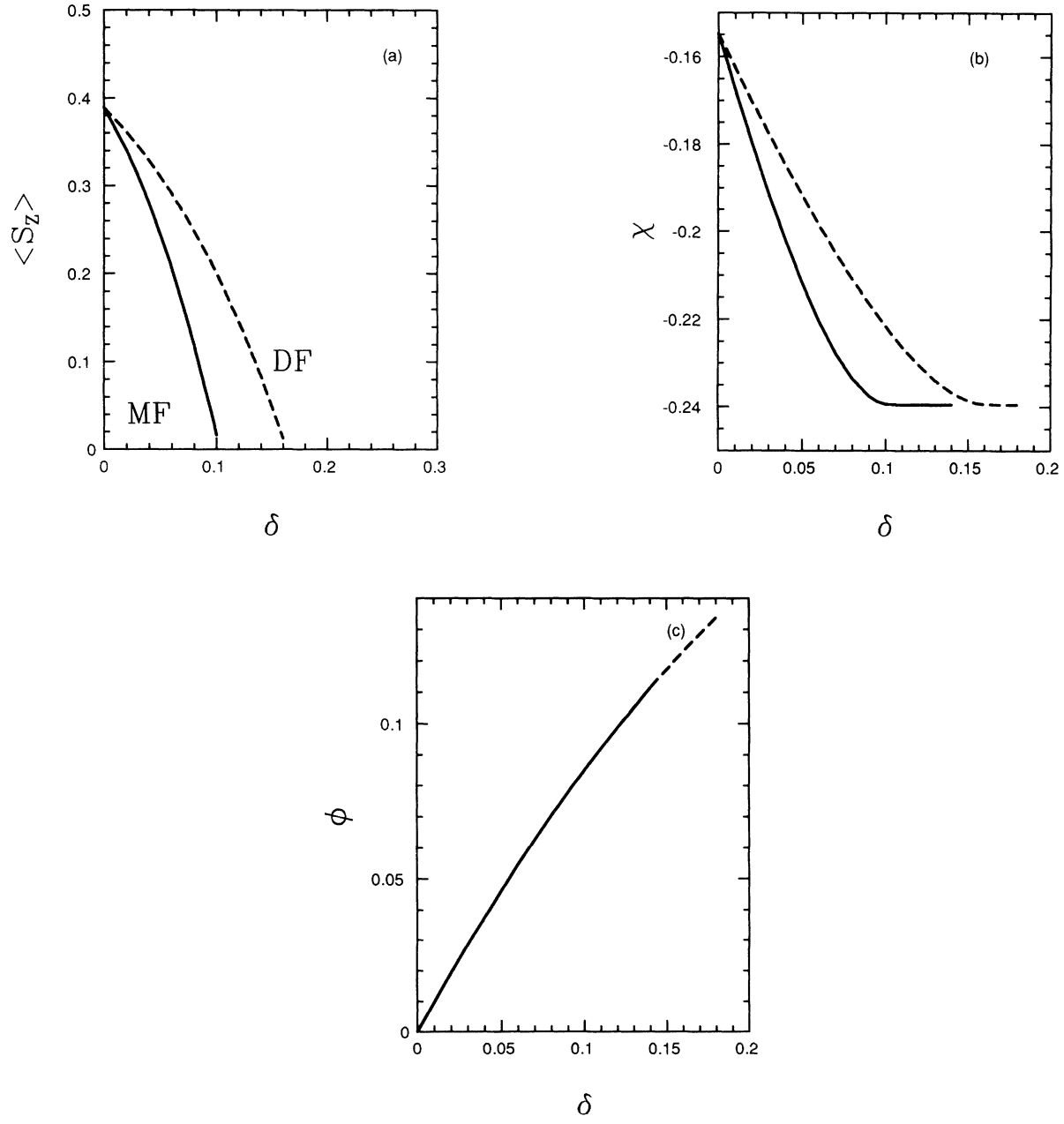

FIG. 4. (a) The staggered magnetization, (b) the orbital current order parameter χ, and (c) the order parameter ϕ as a function of the hole concentration δ, for t/J=5 (solid line) and t/J=3 (dashed line). MF denotes magnetized flux phase with long-range order, while DF is the disordered flux phase.

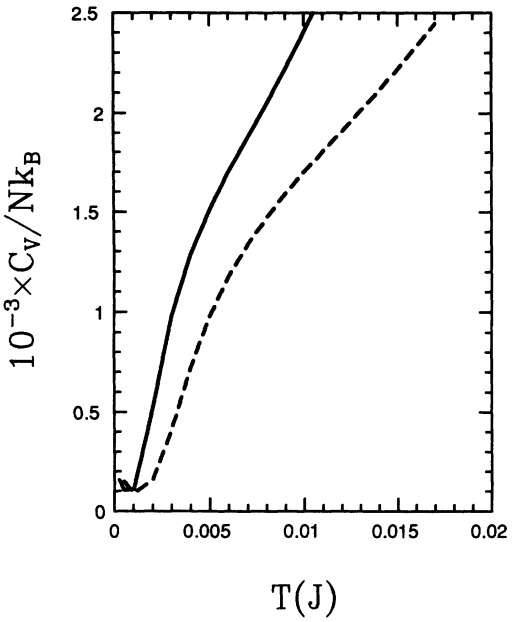

FIG. 5. Specific heat data as a function of temperature T (in units of J) at the hole concentration $\delta = 0.2$ for $t/J = 3$ (solid line) and $t/J = 5$ (dashed line).

VI. SUMMARY AND DISCUSSIONS

In this paper, we have developed a theoretical framework, fermion-spin approach, to study the low-dimensional t-J model. In this approach, the physical electron is decoupled as a product of a spinless fermion (holon) and *hard-core boson* (spinon). The main advantage of this approach is that the on-site local constraints of the t-J model or the large-U limit Hubbard model can be treated exactly in analytical calculations. In this framework, we have shown that the holon behaves like a spinless fermion, while the spinon is neither boson nor fermion, but a *hard-core boson*, and the sum rule for the physical electron is obeyed. This is not true for the conventional slave-particle theories, where the spinon behaves like a boson (slave-boson approach) or a fermion (slave-fermion approach), and the sum rule for the physical electron is not obeyed *within the decoupling scheme.*[24]

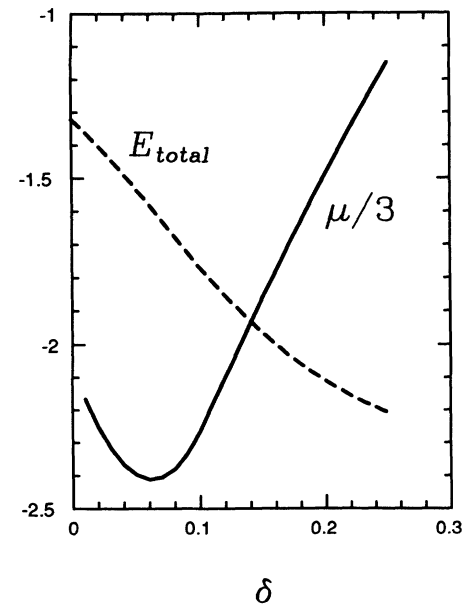

FIG. 6. The total energy $E_{\rm total}$ (dashed line) and the chemical potential $\mu/3$ (solid line) as a function of doping δ for $t/J = 5$. The range of the phase instability is roughly $0 < \delta \leq 0.08$.

We have applied this approach to study the low-dimensional t-J model.

In the 1D case, we have obtained gapless spinon and holon spectra, a good ground state energy, and a reasonable electron-momentum distribution within the MFA. Thus the ground-state in the fermion-spin formalism is in some sense closer to the Bethe-ansatz Lieb-Wu exact wave function of the 1D large-U limit Hubbard model than the slave-particle approach. It is shown that the spinon and consequently also the physical electron behave like Luttinger liquids. We have also obtained the correct asymptotic form of the spin-spin correlation functions as well as the electron-momentum distribution function of the 1D t-J model within the fermion-spin approach by considering the string effects, with results in agreement with the exact numerical simulations of the 1D large-U limit Hubbard model obtained by Ogata and Shiba.[5]

The 1D problem is a good testing ground where the charge and spin are truly separated (not in the literal sense of product of spinon and holon, but rather as independent collective excitations) and the Fermi liquid theory fails to describe its physical properties. To our knowledge, neither the standard perturbation theory nor the conventional slave-particle approach is capable of handling this aspect. Our results of the MFA seem to hint that the fermion-spin approach has some potential to explore further.

The results for 2D are also very encouraging. The magnetized flux phase with a gap proportional to the staggered magnetization, in the spinon excitation spectrum, has the lowest energy at half-filling in the MFA. However, this AFLRO fades away at $10-15\,\%$ hole doping for $t/J = 3-5$, beyond which a gapless flux state becomes stable. This result agrees with experiments and numerical simulations.[49,50,22] It is essential that this mean-field result was obtained without any adjustable parameters. This means that the formalism itself is powerful enough to handle the frustration (delocalization) effect of the t-term in destroying the AFLRO favored by the J-term. However, we should mention that the spin excitation spectrum at half-filling is not gapless in this approach within the MFA as it should be (spin waves). Both Laughlin's approach[43] and Hus's treatment[46] suffer from the same weakness. Probably, it can be cured by including vertex corrections.

As mentioned in Sec. II, this formalism counts doubly the empty site by assigning a "spin" to it. As shown there, this defect can be cured by introducing a projection operator to remove the extra degrees of freedom.

However, in our mean-field treatments we have not taken this projection operator explicitly into account. The fact that we still obtain very good results, as summarized above, indicates that we are not making substantial errors by allowing this extra degree of freedom, at least in problems considered so far.

A natural question is what is the reason why this simple-minded transformation is so useful? To our present understanding, there are at least three reasons: (1) The local constraint is exactly satisfied even at the mean-field level. (2) The *hard-core* nature is kept in the calculation via the Jordan-Wigner transformation in 1D (Ref. 25) or its generalization in 2D.[26] (3) The representation of the *hard-core* boson in terms of spin raising and lowering operators is essential, because whenever a hole hops it gives rise immediately to a change of the spin background as a result of careful treatment of the constraint given in Sec. II B. This is why the t-term is so efficient in destroying the AFLRO. Of course, there are many open questions in this approach, e.g., how to go beyond the MFA, what is the gauge field in this approach, what are its major effects, and so on. These and other related issues are under investigation now.

Recently, we found Ref. 56, where a similar approach was used to study the normal state properties of oxide superconductors. Apart from the difference in issues addressed in our paper and theirs, a careful reader could easily discover the substantial distinction in the interpretation of transformations used in these two papers.

ACKNOWLEDGMENTS

The authors would like to thank P. Fazekas, R. B. Laughlin, N. Nagaosa, A. Parola, S. Sarker, E. Tosatti, G. M. Zhang, and X. Y. Zhang for helpful discussions. S. P. Feng and Z. B. Su would like to thank the ICTP for the hospitality. We thank R. B. Laughlin for bringing Ref. 46 to our attention.

APPENDIX A: MATRIX REPRESENTATION OF THE PROJECTION OPERATOR

The holon operators $h^\dagger$ and h in the basis $\binom{1}{0}_h$, $\binom{0}{1}_h$ of holon states are given by

$$h^\dagger = \begin{pmatrix} 0 & 1 \\ 0 & 0 \end{pmatrix}_h, \quad h = \begin{pmatrix} 0 & 0 \\ 1 & 0 \end{pmatrix}_h, \tag{A1}$$

while the spin raising and lowering operators S^+, S^- in the spin-$\frac{1}{2}$ space $\binom{1}{0}_s$, $\binom{0}{1}_s$ are given by

$$S^+ = \begin{pmatrix} 0 & 1 \\ 0 & 0 \end{pmatrix}_s, \quad S^- = \begin{pmatrix} 0 & 1 \\ 0 & 0 \end{pmatrix}_s. \tag{A2}$$

In the product space $|\text{hole}\rangle \otimes |\text{spin}\rangle$ the basis vectors are

$$|1,\uparrow\rangle = \begin{pmatrix} 1 \\ 0 \end{pmatrix}_h \otimes \begin{pmatrix} 1 \\ 0 \end{pmatrix}_s = \begin{pmatrix} 1 \\ 0 \\ 0 \\ 0 \end{pmatrix},$$

$$|1,\downarrow\rangle = \begin{pmatrix} 1 \\ 0 \end{pmatrix}_h \otimes \begin{pmatrix} 0 \\ 1 \end{pmatrix}_s = \begin{pmatrix} 0 \\ 1 \\ 0 \\ 0 \end{pmatrix},$$

$$|0,\uparrow\rangle = \begin{pmatrix} 0 \\ 1 \end{pmatrix}_h \otimes \begin{pmatrix} 1 \\ 0 \end{pmatrix}_s = \begin{pmatrix} 0 \\ 0 \\ 1 \\ 0 \end{pmatrix},$$

$$|0,\downarrow\rangle = \begin{pmatrix} 0 \\ 1 \end{pmatrix}_h \otimes \begin{pmatrix} 0 \\ 1 \end{pmatrix}_s = \begin{pmatrix} 0 \\ 0 \\ 0 \\ 1 \end{pmatrix}, \tag{A3}$$

which form a complete set.

The fermion-spin transformation defined by Eq. (7) gives the following matrix representation for the fermion operators:

$$C_\uparrow = h^\dagger S^- = \begin{pmatrix} 0 & 1 \\ 0 & 0 \end{pmatrix}_h \otimes \begin{pmatrix} 0 & 0 \\ 1 & 0 \end{pmatrix}_s = \begin{pmatrix} 0 & 0 & 0 & 0 \\ 0 & 0 & 1 & 0 \\ 0 & 0 & 0 & 0 \\ 0 & 0 & 0 & 0 \end{pmatrix},$$

$$C_\downarrow = h^\dagger S^+ = \begin{pmatrix} 0 & 1 \\ 0 & 0 \end{pmatrix}_h \otimes \begin{pmatrix} 0 & 1 \\ 0 & 0 \end{pmatrix}_s = \begin{pmatrix} 0 & 0 & 0 & 1 \\ 0 & 0 & 0 & 0 \\ 0 & 0 & 0 & 0 \\ 0 & 0 & 0 & 0 \end{pmatrix},$$

$$C_\uparrow^\dagger = hS^+ = \begin{pmatrix} 0 & 0 \\ 1 & 0 \end{pmatrix}_h \otimes \begin{pmatrix} 0 & 1 \\ 0 & 0 \end{pmatrix}_s = \begin{pmatrix} 0 & 0 & 0 & 0 \\ 0 & 0 & 0 & 0 \\ 0 & 1 & 0 & 0 \\ 0 & 0 & 0 & 0 \end{pmatrix},$$

$$C_\downarrow^\dagger = hS^- = \begin{pmatrix} 0 & 0 \\ 1 & 0 \end{pmatrix}_h \otimes \begin{pmatrix} 0 & 0 \\ 1 & 0 \end{pmatrix}_s = \begin{pmatrix} 0 & 0 & 0 & 0 \\ 0 & 0 & 0 & 0 \\ 0 & 0 & 0 & 0 \\ 1 & 0 & 0 & 0 \end{pmatrix}. \tag{A4}$$

On the other hand, there are only three physical states in the constrained Hilbert space, namely

$$|0\rangle = \begin{pmatrix} 1 \\ 0 \\ 0 \end{pmatrix}, \quad |\uparrow\rangle = \begin{pmatrix} 0 \\ 1 \\ 0 \end{pmatrix}, \quad |\downarrow\rangle = \begin{pmatrix} 0 \\ 0 \\ 1 \end{pmatrix}. \tag{A5}$$

To remove the extra degrees of freedom in the $|\text{hole}\rangle \otimes |\text{spin}\rangle$ space, we introduce a projection operator P. By requiring $P|1,\uparrow\rangle = P|1,\downarrow\rangle = |0\rangle$, $P|0,\uparrow\rangle = |\uparrow\rangle$, and $P|0,\downarrow\rangle = |\downarrow\rangle$, one can easily find its matrix representation

$$P = \{P_{\kappa\alpha}\} = \begin{pmatrix} 1 & 1 & 0 & 0 \\ 0 & 0 & 1 & 0 \\ 0 & 0 & 0 & 1 \end{pmatrix}, \tag{A6}$$

and its Hermitian conjugation

$$P^{\dagger} = \begin{pmatrix} 1 & 0 & 0 \\ 1 & 0 & 0 \\ 0 & 1 & 0 \\ 0 & 0 & 1 \end{pmatrix}. \tag{A7}$$

Using this projection operator, the electron operators in the restricted Hilbert space are given by

$$\tilde{C}_{i\uparrow} = Ph^{\dagger}S^{-}P^{\dagger} = \begin{pmatrix} 0 & 1 & 0 \\ 0 & 0 & 0 \\ 0 & 0 & 0 \end{pmatrix},$$

$$\tilde{C}^{\dagger}_{i\uparrow} = PhS^{+}P^{\dagger} = \begin{pmatrix} 0 & 0 & 0 \\ 1 & 0 & 0 \\ 0 & 0 & 0 \end{pmatrix},$$

$$\tilde{C}_{i\downarrow} = Ph^{\dagger}S^{+}P^{\dagger} = \begin{pmatrix} 0 & 0 & 1 \\ 0 & 0 & 0 \\ 0 & 0 & 0 \end{pmatrix},$$

$$\tilde{C}^{\dagger}_{i\downarrow} = PhS^{-}P^{\dagger} = \begin{pmatrix} 0 & 0 & 0 \\ 0 & 0 & 0 \\ 1 & 0 & 0 \end{pmatrix}, \tag{A8}$$

as quoted in Eq. (11). It is then straightforward to verify the operator relations quoted in the main text [Eqs. (12) and (13)]. In particular, the hole number operator

$$n_h = \begin{pmatrix} 1 & 0 & 0 \\ 0 & 0 & 0 \\ 0 & 0 & 0 \end{pmatrix} = |0\rangle\langle 0|$$
$$= \frac{1}{2}P(|1\uparrow\rangle\langle 1\uparrow| + |1\downarrow\rangle\langle 1\downarrow|)P^{\dagger}. \tag{A9}$$

The physical meaning of Eq. (A9) is transparent: The empty state should be counted only once, not twice. Since in the mean-field treatment the constraint on the average doping concentration δ is imposed directly on $h^{\dagger}h$, the sum rule for the physical electron is satisfied.

[1] P. W. Anderson, in *Frontiers and Borderlines in Many Particle Physics*, edited by R. A. Broglia and J. R. Schrieffer (North-Holland, Amsterdam, 1987), p. 1; Science **235**, 1196 (1987).

[2] F. C. Zhang and T. M. Rice, Phys. Rev. B **37**, 3759 (1988).

[3] See, e.g., the review L. Yu, in *Recent Progress in Many-Body Theories*, edited by T. L. Ainsworth, C. E. Campbell, B. E. Clenceats, and E. Krotscheck (Plenum, New York, 1992), Vol. 3, p. 157.

[4] P. W. Anderson, Phys. Rev. Lett. **64**, 1839 (1990); **67**, 2092 (1991); **67**, 3844 (1991); Science **256**, 1526 (1992); Phys. Scr. **T42**, 11 (1992).

[5] M. Ogata and H. Shiba, Phys. Rev. B **41**, 2326 (1990); H. Shiba and M. Ogata, Int. J. Mod. Phys. B **5**, 31 (1991); Progr. Theor. Phys. Suppl. **108**, 265 (1992).

[6] P. Schlottmann, Phys. Rev. B **36**, 5777 (1986); P. A. Bares and G. Blatter, Phys. Rev. Lett. **64**, 2567 (1990); N. Kawakami and S. K. Yang, *ibid.* **65**, 2309 (1990).

[7] S. Sorella, A. Parola, M. Parrinello, and E. Tosatti, Europhys. Lett. **12**, 721 (1990); H. Frahm and V. E. Korepin, Phys. Rev. B **43**, 5653 (1991).

[8] A. Parola and S. Sorella, Phys. Rev. Lett. **64**, 1831 (1990).

[9] H. Yokoyama and M. Ogata, Phys. Rev. Lett. **67**, 3610 (1991).

[10] F. F. Assaad and D. Würtz, Phys. Rev. B **44**, 2681 (1991).

[11] C. Stephen and E. J. Mele, Phys. Rev. Lett. **67**, 2080 (1991); Phys. Rev. B **44**, 1360 (1991).

[12] F. D. M. Haldane, Phys. Rev. Lett. **45**, 1358 (1980); Phys. Lett. **81A**, 153 (1981); J. Phys. C **14**, 2585 (1981); J. Solyom, Adv. Phys. **28**, 201 (1979).

[13] R. Valenti and C. Gros, Phys. Rev. Lett. **68**, 2402 (1992); R. R. P. Singh and R. L. Glenister, Phys. Rev. B **46**, 14 313 (1992).

[14] S. Sorella, Phys. Rev. B **46**, 11 670 (1992).

[15] D. Poilblanc, H. J. Schulz, and T. Ziman, Phys. Rev. B **46**, 6435 (1992); **47**, 3268 (1993).

[16] S. Schmitt-Rink, C. M. Varma, and A. E. Ruckenstein, Phys. Rev. Lett. **60**, 2793 (1988); C. L. Kane, P. A. Lee, and N. Read, Phys. Rev. B **39**, 6880 (1989); Z. B. Su, Y. M. Li, W. Y. Lai, and L. Yu, Phys. Rev. Lett. **63**, 1318 (1989).

[17] L. Zhang, J. K. Jain, and V. J. Emery, Phys. Rev. B **47**, 3368 (1993).

[18] See, e.g., the review P. A. Lee, in *High Temperature Superconductivity*, Proceedings of the Los Alamos Symposium, 1989, edited by K. S. Bedell, D. Coffey, D. E. Meltzer, D. Pines, and J. R. Schrieffer (Addison-Wesley, Redwood City, CA, 1990).

[19] L. B. Ioffe and A. I. Larkin, Phys. Rev. B **39**, 8988 (1989); N. Nagaosa and P. A. Lee, Phys. Rev. Lett. **64**, 2450 (1990); P. A. Lee and N. Nagaosa, Phys. Rev. B **46**, 5621 (1992).

[20] W. Marshall, Proc. R. Soc. London, Ser. A **232**, 48 (1955).

[21] S. Liang, B. Doucot, and P. W. Anderson, Phys. Rev. Lett. **61**, 365 (1988).

[22] T. K. Lee and Shiping Feng, Phys. Rev. B **38**, 11 809 (1988).

[23] A. P. Arovas and A. Auerbach, Phys. Rev. B **38**, 316 (1988); D. Yoshioka, J. Phys. Soc. Jpn. **58**, 32 (1989); C. L. Kane *et al.*, Phys. Rev. B **41**, 2653 (1990).

[24] Shiping Feng, J. B. Wu, Z. B. Su, and L. Yu, Phys. Rev. B **47**, 15 192 (1993).

[25] P. Jordan and E. Wigner, Z. Phys. **47**, 631 (1928).

[26] E. Mele, Phys. Scr. **T27**, 82 (1988); E. Fradkin, Phys. Rev. Lett. **63**, 322 (1989); G. Baskaran, in *Two-Dimensional Strongly Correlated Electronic Systems*, edited by Z. Z. Gan and Z. B. Su (Gordon and Breach, New York, 1989), p. 72; J. Ambjorn and G. W. Semenoff, Phys. Lett. **226B**, 109 (1989).

[27] See, e.g., C. Gros, R. Joynt, and T. M. Rice, Phys. Rev. B **36**, 381 (1987).

[28] L. B. Ioffe and P. B. Wiegmann, Phys. Rev. Lett. **65**, 653 (1990); P. B. Wiegmann, *ibid.* **60**, 821 (1988); Physica **153-155C**, 103 (1988).

[29] Z. Y. Weng, D. N. Sheng, C. S. Ting, and Z. B. Su, Phys. Rev. B **45**, 7850 (1992); Phys. Rev. Lett. **67**, 3318 (1991).

[30]J. Hubbard, Proc. R. Soc. London, Ser. A **276**, 238 (1963); **296**, 82 (1966); see, also, F. C. Zhang and T. K. Lee, Phys. Rev. B **28**, 33 (1983).
[31]G. Martinez and P. Horsch, Phys. Rev. B **44**, 317 (1991); F. Marsiglio, A. E. Ruckenstein, S. Schmitt-Rink, and C. M. Varma, *ibid.* **43**, 10 882 (1991).
[32]E. H. Lieb and F. Y. Wu, Phys. Rev. Lett. **20**, 1445 (1968); C. N. Yang, *ibid.* **19**, 1312 (1967).
[33]Z. Wang, Y. Bang, and G. Kotliar, Phys. Rev. Lett. **67**, 2733 (1991); C. A. R. Sá de Melo, Z. Wang, and S. Doniach, *ibid.* **68**, 2078 (1992).
[34]A. Luther and I. Peschel, Phys. Rev. B **12**, 3908 (1975); G. D. Mahan, *Many-Particle Physics* (Plenum, New York, 1981), and references therein.
[35]H. Bethe, Z. Phys. **71**, 205 (1931); L. Hulthén, Arkiv. Mat. Astron. Fys. **26A**, No. 11 (1938).
[36]F. D. M. Haldane, Phys. Rev. Lett. **66**, 1529 (1991).
[37]Y. R. Wang, Phys. Rev. B **43**, 3786 (1991); **46**, 151 (1992), and references therein.
[38]See, e.g., D. J. Klein and W. A. Seitz, Phys. Rev. B **10**, 3217 (1974); U. Brandt, Z. Phys. **269**, 221 (1974).
[39]G. Baskaran, Z. Zou, and P. W. Anderson, Solid State Commun. **63**, 973 (1987).
[40]I. Affleck and J. B. Marston, Phys. Rev. B **37**, 3774 (1988); G. Kotliar, *ibid.* **37**, 3664 (1988).
[41]B. Shraiman and E. Siggia, Phys. Rev. Lett. **62**, 1564 (1989).
[42]P. W. Anderson, B. S. Shastry, and D. Hristopulos, Phys. Rev. B **40**, 8939 (1989); P. Wiegmann, Phys. Rev. Lett. **65**, 2070 (1990); P. Lederer, D. Poilblanc, and T. M. Rice, *ibid.* **63**, 1519 (1989).
[43]V. Kalmeyer and R. B. Laughlin, Phys. Rev. Lett. **59**, 2095 (1987); R. B. Laughlin, Science **242**, 525 (1988); Phys. Rev. Lett. **60**, 2677 (1988); X. Wen, F. Wilczek, and A. Zee, Phys. Rev. B **39**, 11 413 (1989).
[44]D. N. Sheng, Z. B. Su, and L. Yu, Phys. Rev. B **42**, 8732 (1990).
[45]H. Chen, Z. B. Su, and L. Yu, Phys. Rev. B **41**, 267 (1990); G. Khaliullin and P. Horsch, *ibid.* **47**, 463 (1993).
[46]T. C. Hsu, Phys. Rev. B **41**, 11 379 (1990).
[47]M. U. Ubbens and P. A. Lee, Phys. Rev. B **46**, 8434 (1992).
[48]N. Trivedi and D. M. Ceperley, Phys. Rev. B **40**, 2747 (1989).
[49]D. Vaknin *et al.*, Phys. Rev. Lett. **58**, 2802 (1987); J. H. Brewer *et al.*, *ibid.* **60**, 1073 (1988).
[50]Y. Kitaoka *et al.*, Physica **C153-155**, 733 (1988).
[51]Shiping Feng, J. Phys. Condens. Matter **5**, 115 (1993); (unpublished).
[52]See, e.g., the review H. E. Fischer, S. K. Watson, and D. G. Cahill, Comments Condens. Matter Phys. **14**, No. 2, 65 (1988).
[53]P. Gutsmiedl *et al.*, Jpn. J. Appl. Phys. **26**, Suppl. 26-3, 1117 (1987); A. P. Ramirez *et al.*, Phys. Rev. B **35**, 8833 (1987); A. Junod *et al.*, Jpn. J. Appl. Phys. **26**, Suppl. 26-3, 1119 (1989); S. J. Collocott *et al.*, Phys. Rev. B **36**, 5684 (1987); B. D. Dunlap *et al.*, *ibid.* **35**, 7210 (1987); K. Kitazawa *et al.*, Jpn. J. Appl. Phys. Lett. **26**, L751(1987).
[54]V. J. Emery, S. A. Kivelson, and H. Q. Lin, Phys. Rev. Lett. **64**, 475 (1990); S. A. Kivelson, V. J. Emery, and H. Q. Lin, Phys. Rev. B **42**, 6523 (1990).
[55]W. Q. Putikka, M. U. Luchini, and T. M. Rice, Phys. Rev. Lett. **68**, 538 (1992).
[56]Y. R. Wang, J. B. Wu, and M. Franz, Phys. Rev. B **47**, 12 140 (1993).